

Assessment of fixed, single-axis, and dual-axis photovoltaic systems applied to a reverse osmosis desalination process in northwest Mexico

Jorge Rodríguez-López^a, Adriana Robles-Lizárraga^b, María I. Encinas-Guzmán^a, Felipe Correa-Díaz^c, Germán E. Dévora-Isiordia^{b,*}

^aNatural Resources, Instituto Tecnológico de Sonora, Calle 5 de Febrero 818 Sur, Ciudad Obregón, Son., México, Zip Code 85000, emails: jrodl@hotmail.com (J. Rodríguez-López), isela.eg@gmail.com (M.I. Encinas-Guzmán)

^bDepartment of Water and Environmental Sciences, Instituto Tecnológico de Sonora, Calle 5 Febrero 818 Sur, Ciudad Obregón, Son., México, Zip Code 85000, email: adri_354@hotmail.com (A. Robles-Lizárraga), german.devora@itson.edu.mx (G.E. Dévora-Isiordia)

^cFaculty of Marine Science, Universidad Autónoma de Baja California, Carretera Transpeninsular Ensenada-Tijuana 3917, Zip Code 22860, Ensenada, Baja California, México, email: fcorreadiaz@gmail.com

Received 18 November 2020; Accepted 7 July 2021

ABSTRACT

Desalination allows reducing water scarcity problems by means of techniques as reverse osmosis (RO), and currently, its main disadvantage is high energy demand. Therefore, this study assessed energy consumption of a desalination plant by RO with different current concentrations (5,000–36 000 mg/L of total dissolved solids), maintaining a constant feed conversion flux of 14.4 m³/d and 40%. Additionally, three photovoltaic (PV) systems were used as an energy source: fixed, single-axis, and dual-axis trackers. Instantaneous power was recorded from the three PV systems with the purpose of testing if the power energy generated complied with that required by the RO process at different concentrations. An energy productivity simulation was performed by PVsyst V6.75 to validate and compare the data generated by the real system. This study showed the ascending tendency in energy demand with respect to feeding water salinity into the desalination plant where the energy consumption rate went from 2.33 to 3.83 kWh/m³. The dual-axis system showed the greatest energy production. The equation to calculate the obtained energy demand was $R^2 = 0.98$, which should aid the desalination process design for similar sites.

Keywords: Water scarcity; Desalination; Photovoltaic systems; Energy production; Photovoltaic systems

1. Introduction

Water is fundamental for life on Earth and a key factor for the development of humanity. Nonetheless, current hydric resource availability has been affected mainly by demographic growth and overexploitation of the aquifers for economic development, causing scarcity problems to a fifth part of the world population [1,2]. The available water volume at the world level has been estimated to be 1,386 million km³, but only 2.5% (35 million km³) of this resource is freshwater. Nevertheless, almost 70% is frozen

in the Earth poles, which hinders its usage. As a result, only 0.76% of water worldwide is accessible for humanity [3].

In Mexico, water availability varies among the regions that comprise the country. The southeastern region concentrates 67% of renewable water while the northern, central, and northwestern regions have only 33% of available water [4]. The State of Sonora, located in northwest Mexico, has water availability problems mainly caused by high salt concentration in wells (2,000–5,000 mg/L TDS – total dissolved solids). This situation is attributed mainly to salinity intrusion effects caused by overexploitation of aquifers [5].

* Corresponding author.

During the last years, a great number of regions with water scarcity problems have supplied water to their communities by desalination methods, mainly by reverse osmosis (RO) [5,6]. This process has the objective of removing dissolved salt in brackish (1,000–10,000 mg/L TDS) or seawater (30,000–40,000 mg/L TDS) to obtain quality water and satisfy human consumption demand, agricultural irrigation, and industrial processes [3,7].

This method has grown in popularity because it can be applied at small and large scales [8]. However, one of the main problems of the RO processes is their high energy demand, generated principally by fossil fuels linked to environmental deterioration, causing acid rain, greenhouse gas emissions, and climate change [9]. For this reason and constant price increase of such fuels, it is essential to implement systems that function with renewable energies [10].

One of the main advantages of RO desalination is its capacity to adapt itself to coupling renewable energies [11]. Among the different renewable energy sources, solar energy is undoubtedly the one with the greatest accessibility and may be utilized for water desalination without generating greenhouse effects [3]. Northwest Mexico is one of the best sites for the use of solar resources. It maintains high levels of daily solar radiation with an average of 5.5 kWh/m² and the capacity of reaching up to 10 kWh/m² during the day, especially during the spring and summer seasons [12].

To this day, some brackish water desalination facilities powered by photovoltaic (PV) systems are found in countries, such as Brazil, Egypt, Spain, and Iraq [11]. The RO desalination plants that function through PV panels are excellent to make water drinkable in small communities that aren't grid-connected but have brackish, saline or seawater access. This type of small-scale facility represents a greater cost-benefit facing other technologies [13].

The viability of PV systems in RO desalination processes depends on several factors, such as variation of solar radiation, type of water source used, and system size. Despite current investigations, solar energy and desalination continue being research areas in development, boosted by the need to reduce energy consumption [14].

To improve photovoltaic panel efficiency, solar tracking systems should be implemented; they allow the collector surface to be perpendicular to the sun rays, thus capturing a greater amount of direct solar radiation and increasing electricity production [15].

Therefore, the objective of this study is to evaluate the energy consumption of a desalination plant by reverse osmosis with feed flux and constant conversion at different salinities. For this purpose, three different solar panel photovoltaic systems were used as a source of energy (fixed, single-axis and dual-axis trackers).

2. Materials and methods

2.1. Location of the study area

Seawater sampling was performed along the coast of the Gulf of California, in the port of Guaymas, Sonora, México with the following coordinates 27° 55' 18.83" N and 110° 56' 59.43" E (Fig. 1). Approximately, 600 L of seawater of 36,000 mg/L TDS were collected.

2.2. Feedwater

Five different water sources to be desalinated were prepared. Seawater (36,000 mg/L TDS) and the rest 5,000; 10,000; 15,000 and 20,000 mg/L TDS mixing seawater and tap water (208 mg/L TDS). The amounts to be mixed were determined by the following equation:

$$C_1V_1 + C_2V_2 = C_fV_f \quad (1)$$

2.3. Desalination plant operation

A RO desalination plant with a capacity of 5.76 m³/d was operated, composed of four commercial membranes (Hydranautics, Model SWC4-MAX^a) 8" × 40" connected in parallel-series to desalinate five water treatments at different concentrations (Fig. 2). This membrane had a permeation flow of 27.3 m³/d, salt rejection of 99.8%, an equivalent area of 40.9 m² and a maximum pressure of 8.27 MPa. These yields apply in standardized testing conditions (32,000 ppm, 5.5 MPa, 10% conversion, 25°C pH 6.5–7). This equipment does not have an energy recovery device.

The pretreatment was composed of sand and activated carbon filters with capacities of 2.12 m³ in both cases. Subsequent to the previous equipment, a salt softener was coupled with the same capacity and a 5 μm cartridge filter. At the same time, water post-treatment was performed with ultraviolet (UV) rays (WEDECO UV Technologies Inc., Model NLR1845WS).

During the desalination procedure, an antiscalant agent (Vitec 4000) was added to the feed with an injection pump to minimize membrane polarization by salt incrustation and fouling effect [16,17]. The conversion rate was 40% for all treatments.

2.4. Measurement of water quality parameters and salt rejection

Field water quality parameters were measured at the end of each experimental run with a YSI 556 multiparametric equipment, which was electrical conductivity (mS/cm), TDS (mg/L), pH and temperature (°C). Measurements were performed in triplicate, and the corresponding descriptive statistics were performed for data processing.

To calculate salt rejection percentage, the following formula was used [18]:

$$\%R = \left[\frac{(C_f - C_p)}{C_f} \right] \times 100 \quad (2)$$

2.5. Different photovoltaic system arrangement

The required energy demand by the desalination plant fed with different concentrations was provided by three different PV systems trackers: fixed, single-axis, and dual-axis. Each system had 24 PV panels. In total for this research, 72 PV polycrystalline REC solar, Model REC240PE (BLK), REC Peak Energy Series Black (NO) and 72 micro-inverters (ENPHASE Model M215-60-2LL-S22) were used. Tables 1 and 2 show the characteristics of panel

and inverter models, respectively. When energy generation is greater than each treatment demand, energy in excess is provided to a research building where the desalination plant of this study – interconnection network system – is found.

2.6. Energy productivity record of the photovoltaic systems

Energy production (kWh) of the three PV systems was recorded simultaneously and instantaneous reading intervals daily each 30 min by the “Enlighten Manager” (<https://enlighten.enphaseenergy.com>). The period for measuring and obtaining data was from March 13th – August 30th, 2018.

2.7. Approximate energy production projection of the photovoltaic solar system

The software PVsyst ver. V6.75 was used to compare generated data vs. simulated data. The characteristics of panel and inverter models installed in the three PV systems were entered in the program. Additionally, the study

site coordinates were also entered for simulation and analysis of the PV installation data. Energy losses caused by temperature increase, inverter efficiency, and shading by adjacent objects were also considered.

2.8. Determining energy consumption of the desalination plant

To determine the energy demand of the desalination plant utilizing water at different concentrations, the energy

Table 1
Technical characteristics of the PV panel REC240PE (BLK)

Electrical parameters	Value
Nominal power (W)	240
Nominal power voltage (V)	30.4
Nominal power current (A)	7.9
Open circuit voltage (V)	37.7
Short circuit current (A)	8.4
Nominal operating cell temperature (°C)	45.7
Module efficiency (%)	14.5
Cell number	60

<https://www.technosun.com/descargas/REC-PE-235-240-245-250-255-260-ficha-EN.pdf>

Table 2
Technical characteristics of microinverter Model M215-60-2LL-S22

Electrical parameters	Value
Recommended maximum input power (W)	190–270
Maximum input DC voltage (V)	48
Maximum output power (W)	215
Nominal frequency (Hz)	60
Operating temperature range (°C)	–40–65
Peak inverter efficiency (%)	96.5

<https://d1819pwkf4ncw.cloudfront.net/files/documents/enphasem215datasheet1-43765.pdf>

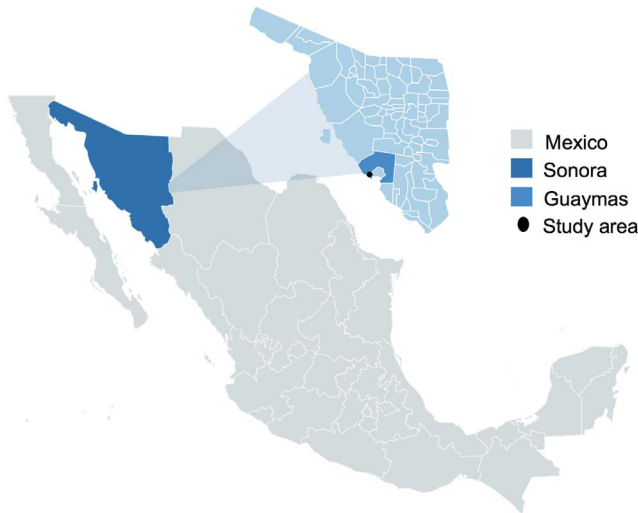


Fig. 1. Area of study in Guaymas, Sonora, Mexico (Source: Robles, 2019).

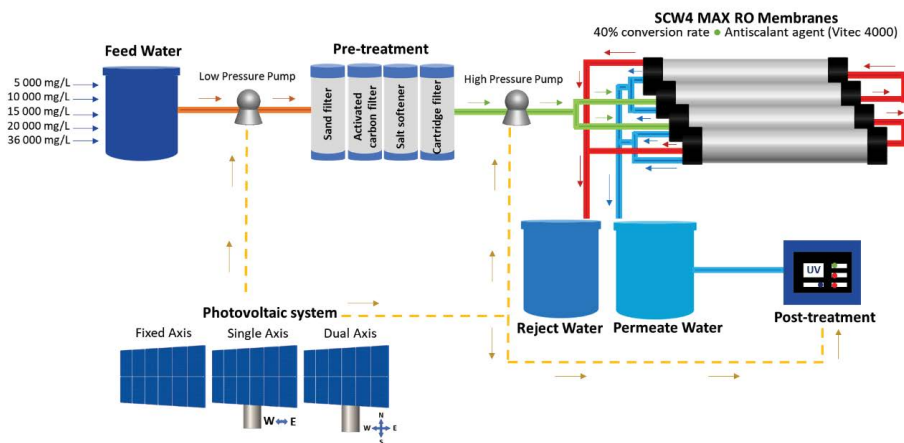


Fig. 2. Diagram of reverse osmosis (RO) desalination plant. SWC4-MAX: <https://membranes.com/wp-content/uploads/2017/03/SWC4-MAX.pdf>

consumption of the complete system was recorded. A standard multifunction energy counter Delta Model DPM-C520 was used for the high-pressure pump. System operation time was 15 min in all cases. Energy consumption was calculated and projected at kWh/d with the intention of simulating a RO desalination plant operating 24 h a day with an input flow of 14.4 m³/d.

2.9. Obtaining the equation to estimate energy consumption

To analyze the relationship between treated water salinity and energy consumption of the desalination plant, an equation was used to estimate the energy demand required by a RO desalination process at any salinity within the range in the study (5,000–36,000 mg/L TDS) by linear regression analysis.

3. Results and discussion

3.1. Physical-chemical characteristics of sampling water

Table 3 shows the volume and characteristics of seawater sampled on the coast of Guaymas, Sonora, México. The TDS (mg/L) value agreed with the study of Anis et al. [19] and Kress [20] reporting that seawater salinity may vary depending on the region from 30,000 mg/L up to 40,000 mg/L TDS.

3.2. Water quality

In all the processes, the feedwater temperature was maintained from 21°C–23°C below 27°C, which was recommended [21] for membrane care in a RO system for seawater desalination (Fig. 3). On the other hand, the temperature on salt rejection increased in all the treatments

because of friction and pressure applied to feed water passing through the RO membranes [22]. A decrease in pH was also observed in permeate and rejection processes due to ion and cation removal with respect to feeding flow and the application of acid anti-fouling [23,24].

Since the flow rate of freshwater produced is constant for all the tests, pressure increases with feed salinity, where 0.965 MPa was the lowest value for 5,000 mg/L TDS and 3.792 MPa with respect to seawater concentration of 36,000 mg/L TDS. These results agreed with those reported by the study of Park and Kwon [25], who mentioned that operating pressure in RO desalination processes is reduced with low salinity feed flow.

3.3. Energy demand of the process

The amount of energy required by the plant equipment varied in each one of the five treatments. Energy consumption and energy demand projection at 24 h are shown in Table 5, where an ascending tendency is observed in the energetic requirement as salinity increased in feed water to the desalination plant. This result agreed with that reported by the study of Ahdab et al. [26], who also pointed out

Table 3
Seawater characteristics and volume

Parameter	Value
Volume (L)	600
pH	8.01
Temperature (°C)	21.33
Conductivity (mS/cm)	55.96
TDS (mg/L)	36,000

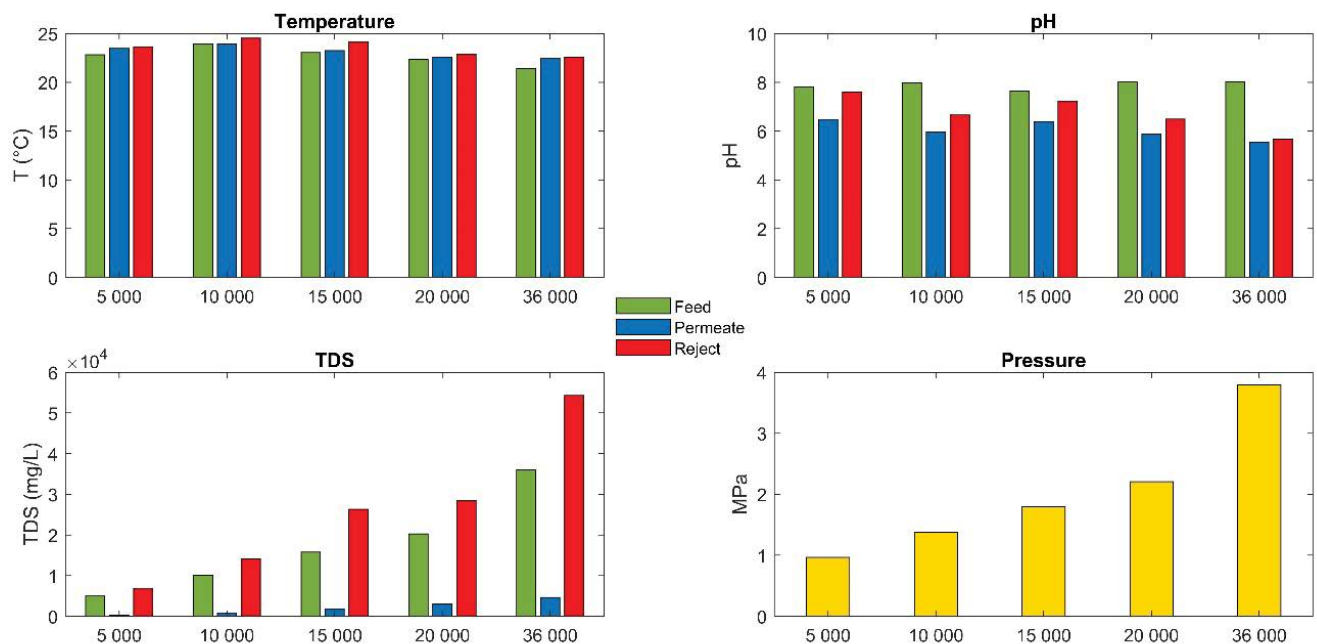


Fig. 3. Water quality and operating pressure.

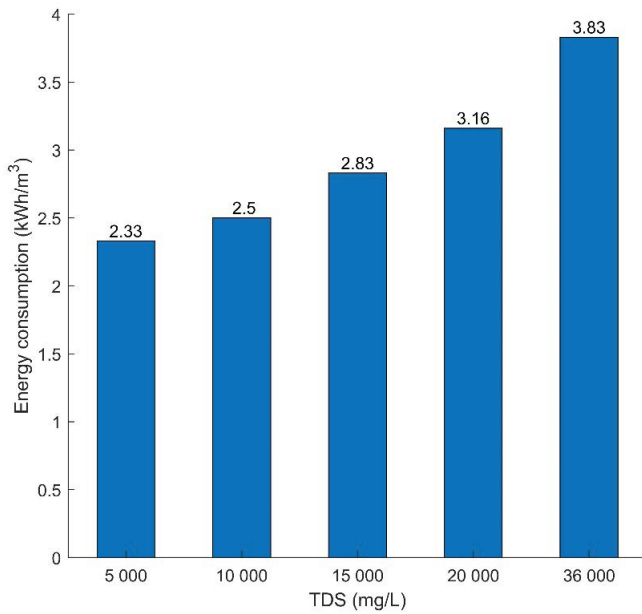


Fig. 4. Energy consumption in kWh/m³.

that the conversion percentage and salinity process had a direct bearing on the energy demand of the desalination plant.

The permeate flow of the desalination plant maintained a water volume of 5.76 m³/d for all treatments since a fixed feed and conversion flow was maintained. As for the energy demand (kWh/m³), as expected, an increase was obtained when water salinity increased (Fig. 4). This result occurred because the low salt concentration in feed flow requires a lower applied pressure, so the energy demand of the process decreases. However, this situation does not apply in RO systems that require greater power for high salinity feed [6].

Table 4
Energy demand with respect to salinity flow

Feed water concentration (mg/L TDS)	Pressure (MPa)	Power (kW)
5,000	0.965	0.064
10,000	1.379	0.092
15,000	1.793	0.120
20,000	2.206	0.147
36,000	3.792	0.253

Table 5
Energy demand projection per daily treatment

TDS (mg/L)	5,000	10,000	15,000	20,000	36,000
Operation time (min)	15	15	15	15	15
Energy consumption per treatment (kWh)	0.14	0.15	0.17	0.19	0.23
Daily energy consumption (kWh/d)	13.44	14.40	16.32	18.24	22.08

3.4. Energetic productivity recorded in photovoltaic systems

Fig. 5 shows the amount of energy produced by each PV system report.

The solar tracking systems, both single-axis and dual-axis, produced greater energy than the fixed system. Maximum energy production in the tracking systems was recorded on day 67 (05/18/2018) since it was a clear day that allowed greater solar radiation capture. This result agreed with the study of Arreola-Gómez et al. [15] who mentioned that when the tracking system was used, the total energy received in one clear day could increase from 35% to 40% compared to a fixed system.

On the other hand, in the history of the 172-d study, at least 12 events were recorded where energy yield was very similar and with low production for the three photovoltaic systems, which were cloudy days or with low direct radiation. This result agreed with several studies, which demonstrated that the energy yield of a photovoltaic system depended greatly on the amount of clouds, as well as on other factors, such as solar radiation, environmental temperature, the average temperature of the PV panel, and wind speed [27,28]. The accumulated production record of each PV system is shown in Table 6.

Fig. 6 compares energy production hours vs. the power required to desalinate the five treatments, March 13th, 2018 – winter.

The treatment that showed the greatest power (0.253 kW) was the one with 36,000 mg/L TDS; in this sense, all the treatments complied with the reverse osmosis operation in schedule from 09:30 to 16:30 h. On the other hand, if the operation is considered at different hours, the use of technologies should be considered. For example, adding batteries provide missing energy [29] or seasonal water storage tanks in the long term, whose objective is to store excessive water accumulation in high provision periods and supply accumulated water to low production demand during the whole year [30]. These two options have been considered to optimize water production, but they increase investment and require a feasibility study.

3.5. Results generated by the photovoltaic system software report

The real energy production results and those calculated by PVsyst V6.75 for the three PVsyst are shown in Fig. 7.

The greatest power generation – both in simulation and real production – corresponded to the dual-axis system with the peak in May 2018 compared with the fixed and single-axis systems. This production increase could be explained because the dual-axis system allowed a

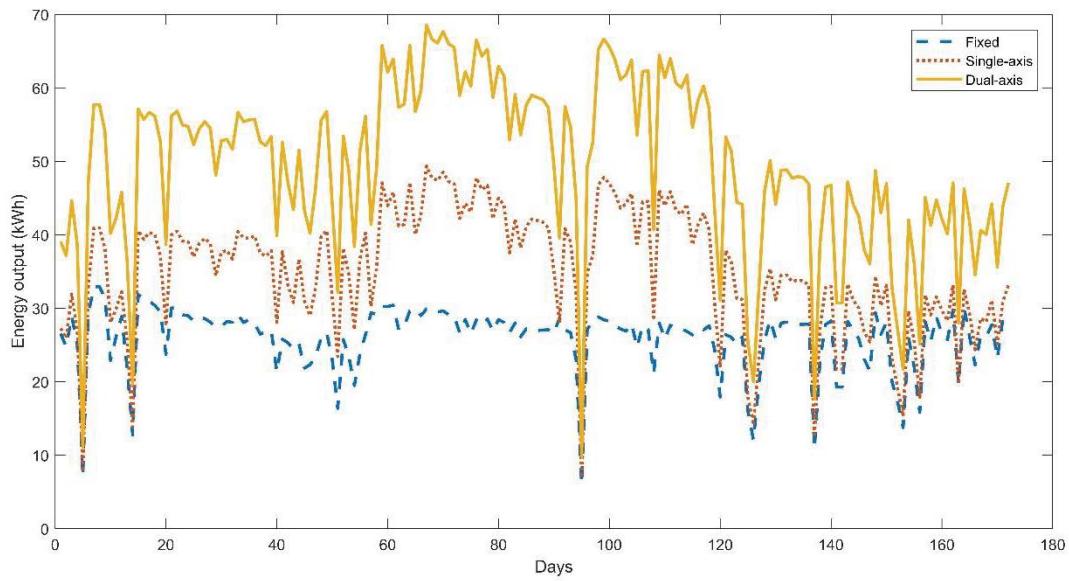


Fig. 5. Energy production record.

Table 6
Record of accumulated energy production per system

Photovoltaic system	Average (kWh/d)	Standard deviation (kWh/d)	Maximum (kWh/d)	Minimum (kWh/d)	Total accumulated energy (kWh)
Fixed-axis	26.04	4.35	32.93	6.04	4,480.38
Single-axis	35.21	8.45	49.33	6.93	6,056.09
Dual-axis	49.52	11.67	68.52	9.79	8,518.66

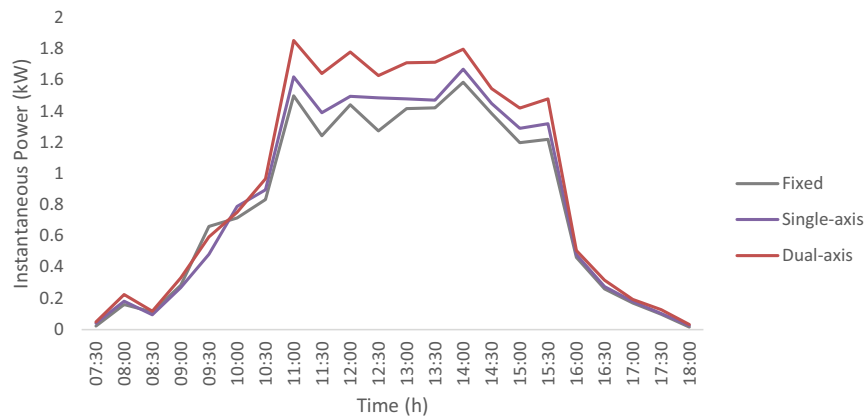


Fig. 6. Instantaneous power per photovoltaic system.

more exact tracking of the sun trajectory and received greater solar radiation incidence in their modules [31,32]. The difference between real and simulated production is attributable to the PVSyst software database that manages monthly averages.

3.6. Loss by shading, temperature and inverter

Loss by shading, temperature and inverter are shown in Fig. 8. The greatest loss by shading was recorded in

the fixed system since it received partial shading of close objects due to its positioning. The previous result agrees with the study of Mohammadi et al. [33], who mentioned that shading of partial PV panels may cause outlet power reduction of the system due to less solar light intensity. This result may be due to different factors, such as clouds, shades of trees, buildings, or other objects close by. Thus, the importance of taking into account all shades from the moment of installing the equipment, including those generated by relatively small obstacles.

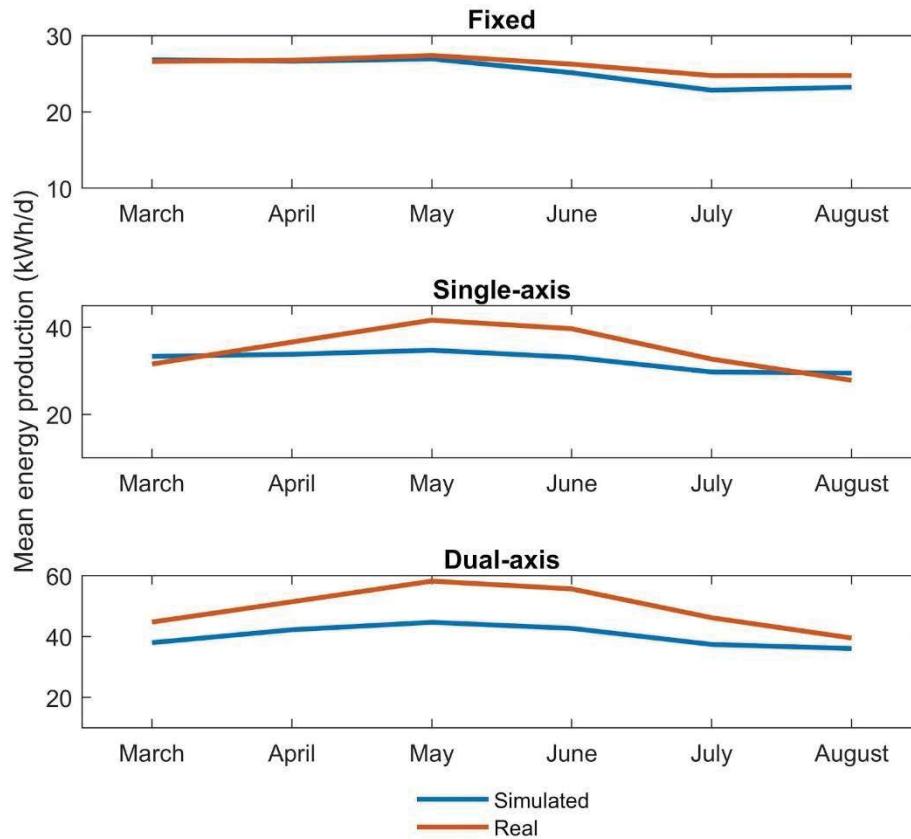


Fig. 7. Real energy production vs. simulated production (PVsyst V6.75).

On the other hand, the greatest loss due to the temperature effect was recorded in the dual-axis system because it maintained greater direct radiation during most of the day by following the sun in its axes N-S, E-W. Besides, the efficiency of the PV system depends on temperature and solar power [34]. These results agree with that reported by

the study of Hammad et al. [35], who mentioned that photovoltaic panel power and efficiency decreased between 0.5% and 0.005%/°C, as environmental temperature increased. Regarding the inverter, when dealing with the same model, the loss percentage was maintained constant in the three systems.

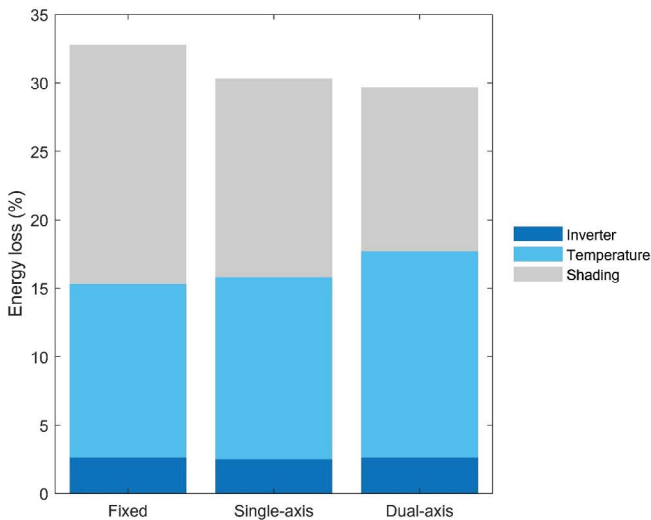


Fig. 8. Loss due to temperature, shading, and inverter.

3.7. Projection equation for energy consumption

The relationship between salinity and water and the amount of electricity for each treatment is shown in Fig. 9.

Eq. (3) was obtained in order to calculate the required energy demand for the RO desalination process at any salinity concentration within the range in the study (5,000–36,000 mg/L TDS). The correlation coefficient value (R^2) was 0.98; since osmotic pressure increases linearly with salinity when the permeate water flow is maintained constant, the pressure difference must be constant.

$$E = 0.0002C_f + 24.505 \tag{3}$$

Obtaining a projection model of energy demand in a desalination plant is greatly important to be able to estimate different factors, such as plant size, installation and production costs. This facilitates the design and quote of the necessary infrastructure for current and future projects. Previous researches have confirmed the socioeconomic feasibility to develop desalination processes that operate in

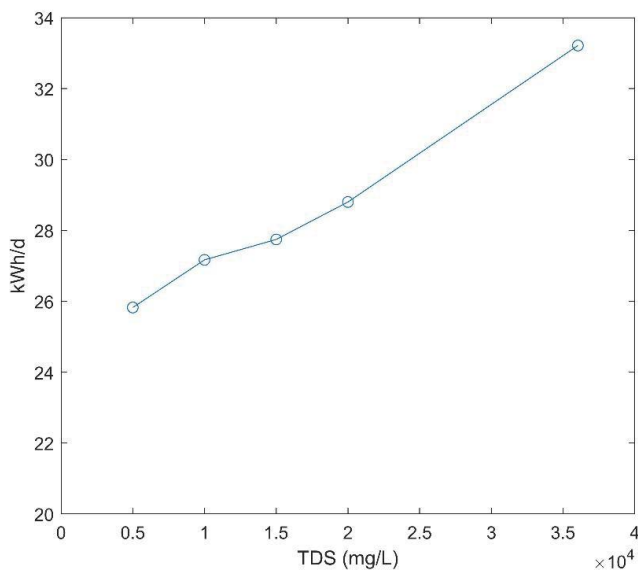


Fig. 9. Relationship between salinity and energy demand.

rural areas. However, a continuous plant operation (24 h/d) requires coupling batteries to function at night which would increase operation cost or design osmosis and energy production processes at effective solar hours on-site [11].

4. Conclusions

The results obtained in this research demonstrated that an ascending tendency exists in operation pressure with respect to feed water salinity in the RO plant, this goes from 0.965 MPa (5,000 mg/L TDS) to 3.792 MPa (36,000 mg/L TDS). The energy consumption process was maintained from 2.33 to 3.83 kWh/d.

Total energy generation was 4,480.38, 6,056.09 and 8,518.66 kWh for the fixed, single-axis, and dual-axis tracking systems in the 172-day period of study with differences between recorded and simulated production of 3.76%, 11.46%, and 22.2%, respectively. The accumulated generation of the three systems was 19 055.14 kWh. The PV dual-axis tracking system was the one with the greatest potential – both in real as in simulated production by the PVsyst software, reaching a maximum production of 58.17 and 44.65 kWh/d, respectively, in May 2018.

The instantaneously generated power did not always reach the desalination of the treatments in the study due to hourly radiation, which demonstrated the need for pressure control of the osmosis operating system, without risking permeated water quality.

Temperature increase in the PV modules was the main cause of energy production loss for the single and dual-axis systems (13.3% and 15.1%, respectively, whereas shading was the main cause of loss (17.5%) for the fixed system.

The equation to estimate energy demand of the RO desalination process obtained a correlation index of $R^2 = 0.98$, greatly easing the design of PV systems found in similar radiation conditions to those in this study. The State of Sonora suffers from water scarcity and meets the favorable

climatological qualities for installing water desalination systems with PV solar energy coupling. Therefore, this entity is an ideal site for research and implementation of these technologies that promote attention to national water and energy problems. The constant advance in the scientific community will lead eventually to never lack an essential resource, such as water.

Acknowledgments

The authors are grateful to Diana Fischer for translation and edition; Instituto Tecnológico de Sonora for financing resources through the research support program (PROFAPI) to publish this manuscript.

Symbols

C_1	–	Tap water concentration, mg/L TDS
C_2	–	Seawater concentration, mg/L TDS
C_f	–	Feed water concentration, mg/L TDS
C_p	–	Permeate concentration, mg/L TDS
V_1^p	–	Tap water volume, L
V_2^p	–	Seawater volume, L
V_3^p	–	Feed water volume, L
%R	–	Rejection percentage
E	–	Energy demand, kWh/d

References

- [1] S. Manju, N. Sagar, Renewable energy integrated desalination: a sustainable solution to overcome future fresh-water scarcity in India, *Renewable Sustainable Energy Rev.*, 73 (2017) 594–609.
- [2] J.A. Aznar-Sánchez, L.J. Belmonte-Ureña, J.F. Velasco-Muñoz, F. Manzano-Agugliaro, Economic analysis of sustainable water use: a review of worldwide research, *J. Cleaner Prod.*, 198 (2018) 1120–1132.
- [3] M. Sarai Atab, A.J. Smallbone, A.P. Roskilly, A hybrid reverse osmosis/adsorption desalination plant for irrigation and drinking water, *Desalination*, 444 (2018) 44–52.
- [4] J. Godínez Madrigal, P. van der Zaag, N. van Cauwenbergh, A half-baked solution: drivers of water crises in Mexico, *Proc. Int. Assoc. Hydrol. Sci.*, 376 (2018) 57–62.
- [5] G.E. Dévora-Isiordia, M.E. López-Mercado, G.A. Fimbres-Weihs, J. Álvarez-Sánchez, J.S. Astorga-Trejo, Desalación por ósmosis inversa y su aprovechamiento en agricultura en el valle del Yaqui [Desalination by reverse osmosis and its use in agriculture in Valle Del Yaqui, Sonora, Mexico], *Sonora, México, Water. Sci. Technol.*, 7 (2018) 155–169.
- [6] N. Ghaffour, T.M. Missimer, G.L. Amy, Technical review and evaluation of the economics of water desalination: current and future challenges for better water supply sustainability, *Desalination*, 309 (2013) 197–207.
- [7] G.E. Dévora-Isiordia, R. González-Enríquez, S. Ruiz-Cruz, Evaluación de procesos de Desalinización y su desarrollo en México [Evaluation of desalination processes and their development in Mexico], *Water Sci. Technol.*, 4 (2013) 27–46.
- [8] M.A. Al-Obaidi, A.A. Alsarayreh, A.M. Al-Hroub, S. Alsaide, I.M. Mujtaba, Performance analysis of a medium-sized industrial reverse osmosis brackish water desalination plant, *Desalination*, 443 (2018) 272–284.
- [9] S. Shaaban, H. Yahya, Detailed analysis of reverse osmosis systems in hot climate conditions, *Desalination*, 423 (2017) 41–51.
- [10] G.S. Alemán-Nava, V.H. Casiano-Flores, D.L. Cárdenas-Chávez, R. Díaz-Chavez, N. Scarlat, J. Mahlknecht, J.-F. Dallemand, R. Parra, Renewable energy research progress in Mexico: a review, *Renewable Sustainable Energy Rev.*, 32 (2014) 140–153.

- [11] M.A. Alghoul, P. Poovanaesvaran, M.H. Mohammed, A.M. Fadhil, A.F. Muftah, M.M. Alkilani, K. Sopian, Design and experimental performance of brackish water reverse osmosis desalination unit powered by 2 kW photovoltaic system, *Renewable Energy*, 93 (2016) 101–114.
- [12] A. Domínguez, R. Geyer, Photovoltaic waste assessment in México, *Resour. Conserv. Recycl.*, 127 (2017) 29–41.
- [13] N. Ahmad, A.K. Sheikh, P. Gandhidasan, M. Elshafie, Modeling, simulation and performance evaluation of a community scale PVRO water desalination system operated by fixed and tracking PV panels: a case study for Dhahran city, Saudi Arabia, *Renewable Energy*, 75 (2015) 433–447.
- [14] F.E. Ahmed, R. Hashaikheh, N. Hilal, Solar powered desalination – technology, energy and future outlook, *Desalination*, 453 (2019) 54–76.
- [15] R. Arreola-Gómez, A. Quevedo-Nolasco, M. Castro-Popoca, Á. Bravo-Vinaja, D. Reyes-Muñoz, Diseño, construcción y evaluación de un sistema de seguimiento solar para un panel fotovoltaico [Design, construction and evaluation of a solar tracking system for a photovoltaic panel], *Rev. Mex. Cienc. Agric.*, 6 (2015) 1715–1727.
- [16] A. Sweity, T.R. Zere, I. David, S. Bason, Y. Oren, Z. Ronen, M. Herzberg, Side effects of antiscalants on biofouling of reverse osmosis membranes in brackish water desalination, *J. Membr. Sci.*, 481 (2015) 172–187.
- [17] N. Belkin, E. Rahav, H. Elifantz, N. Kress, I. Berman-Frank, The effect of coagulants and antiscalants discharged with seawater desalination brines on coastal microbial communities: a laboratory and *in situ* study from the southeastern Mediterranean, *Water Res.*, 110 (2017) 321–331.
- [18] J. Kucera, *Reverse Osmosis*, 2nd ed., Scrivener Publishing, Massachusetts, USA, 2015.
- [19] S.F. Anis, R. Hashaikheh, N. Hilal, Reverse osmosis pretreatment technologies and future trends: a comprehensive review, *Desalination*, 452 (2019) 159–195.
- [20] N. Kress, *Desalination Technologies*, K. Nurit, Ed., Marine Impacts of Seawater, Massachusetts, USA, 2019, pp. 11–34.
- [21] Z.K. Al-Bahri, W.T. Hanbury T. Hodgkiess, Optimum feed temperatures for seawater reverse osmosis plant operation in an MSF/SWRO hybrid plant, *Desalination*, 138 (2001) 335–339.
- [22] A. Panagopoulos, K.-J. Haralambous, M. Loizidou, Desalination brine disposal methods and treatment technologies – a review, *Sci. Total Environ.*, 693 (2019) 133545, doi: 10.1016/j.scitotenv.2019.07.351.
- [23] N. Voutchkov, *Desalination Engineering: Planning and Design*, McGraw-Hill, New York, USA, 2013.
- [24] H.-G. Park, Y.-N. Kwon, Investigation on the factors determining permeate pH in reverse osmosis membrane processes, *Desalination*, 430 (2018) 147–158.
- [25] K. Park, J.B. Kim, D.R. Yang, S.W. Hong, Towards a low-energy seawater reverse osmosis desalination plant: a review and theoretical analysis for future directions, *J. Membr. Sci.*, 595 (2020) 117607, doi: 10.1016/j.memsci.2019.117607.
- [26] Y.D. Ahdab, G.P. Thiel, J.K. Böhlke, J. Stanton, J.H. Lienhard, Minimum energy requirements for desalination of brackish groundwater in the United States with comparison to international datasets, *Water Res.*, 141 (2018) 387–404.
- [27] J.F. Armendariz-Lopez, A. Luna-Leon, M.E. Gonzalez-Trevizo, A.P. Arena-Granados, G. Bojorquez-Morales, Life cycle cost of photovoltaic technologies in commercial buildings in Baja California, Mexico, *Renewable Energy*, 87 (2016) 564–571.
- [28] P.M. Rodrigo, R. Velázquez, E.F. Fernández, DC/AC conversion efficiency of grid-connected photovoltaic inverters in central Mexico, *Sol. Energy*, 139 (2016) 650–665.
- [29] B. Rahimi, H. Shirvani, A.A. Alamolhoda, F. Farhadi, M. Karimi, A feasibility study of solar-powered reverse osmosis processes, *Desalination*, 500 (2021) 114885, doi: 10.1016/j.desal.2020.114885.
- [30] T.A. Ajiwiguna, G.-R. Lee, B.-J. Lim, S.-H. Cho, C.-D. Park, Optimization of battery-less PV-RO system with seasonal water storage tank, *Desalination*, 503 (2021), doi: 10.1016/j.desal.2021.114934.
- [31] S. Seme, G. Srpčič, D. Kavšek, S. Božičnik, T. Letnik, Z. Praunseis, B. Štumberger, M. Hadžiselimović, Dual-axis photovoltaic tracking system – design and experimental investigation, *Energy*, 139 (2017) 1267–1274.
- [32] C.A. Arancibia-Bulnes, R. Peón-Anaya, D. Riveros-Rosas, J.J. Quiñones, R.E. Cabanillas, C.A. Estrada, Beam solar irradiation assessment for Sonora, México, *Energy Procedia*, 49 (2014) 2290–2296.
- [33] A. Mohammedi, N. Mezzai, D. Rekioua, T. Rekioua, Impact of shadow on the performances of a domestic photovoltaic pumping system incorporating an MPPT control: a case study in Bejaia, North Algeria, *Energy Convers. Manage.*, 84 (2014) 20–29.
- [34] S. Seme, K. Sredenšek, B. Štumberger, M. Hadžiselimović, Analysis of the performance of photovoltaic systems in Slovenia, *Sol. Energy*, 180 (2019) 550–558.
- [35] B. Hammad, M. Al-Abed, A. Al-Ghandoor, A. Al-Sardeah, A. Al-Bashir, Modeling and analysis of dust and temperature effects on photovoltaic systems' performance and optimal cleaning frequency: Jordan case study, *Renewable Sustainable Energy Rev.*, 82 (2018) 2218–2234.